Eur. Phys. J. D **9**, 211–215 (1999)

THE EUROPEAN PHYSICAL JOURNAL D

EDP Sciences

Structure and thermal stability of gold nanoclusters: The Au_{38} case

I.L. Garzón[1], K. Michaelian[1], M.R. Beltrán[2], A. Posada-Amarillas[3], P. Ordejón[4], E. Artacho[5], D. Sánchez-Portal[5], and J.M. Soler[5]

[1] Instituto de Física, Universidad Nacional Autónoma de México, Apartado Postal 20-364, México, D.F., 01000 México
[2] Instituto de Investigaciones en Materiales, Universidad Nacional Autónoma de México, Apartado Postal 70-360, México, D.F., 04510 México
[3] Centro de Investigación en Física, Universidad de Sonora, Apartado Postal 5-088, Hermosillo, Sonora, 83000, México
[4] Departamento de Física, Universidad de Oviedo, Calle Calvo Sotelo s/n, E-33007 Oviedo, Spain
[5] Departamento de Física de la Materia Condensada C-III, Universidad Autónoma de Madrid, E-28049 Madrid, Spain

Received: 1 September 1998 / Received in final form: 14 January 1999

Abstract. Gold nanoclusters with disordered and ordered structures are obtained as the lowest-energy configurations of the cluster potential energy surface (PES) by unconstrained dynamical and genetic/symbiotic optimization methods using an n-body Gupta potential and first-principle calculations [Phys. Rev. Lett. **81**, 1600 (1998)]. In this paper, we report the distribution of lowest-energy minima which characterize the PES of the Au_{38} cluster, and a comparison of structural and thermal stability properties among several representative isomers is presented. Coexistence among different cluster isomeric structures is observed at temperatures around 250 K. The structure factor calculated from the most stable (lowest-energy) amorphous-like cluster configuration is in better agreement with the X-ray powder-diffraction experimental measurements than those calculated from ordered structures.

PACS. 36.40.-c Atomic and Molecular Clusters – 36.40.Cg Electronic Properties of Clusters – 61.46.+w Clusters, Nanoparticles and Nanocrystalline Materials

1 Introduction

Recent advances in the growth of Au clusters reveal the formation of stable gold nanocrystalline assemblies [1]. Mass spectroscopy measurements show the formation of Au clusters of critical sizes at the cores of these samples [2]. Structural characterization and optical absorption studies have been performed for gold clusters in the size range of 1–2 nm (40–200 Au atoms) [3]. Several theoretical approaches are currently available for the study of the physical and chemical behavior of clusters of these sizes [4–7]. In particular, the study of structural properties of gold nanoclusters of these sizes and their interplay with other physical (electronic, optical, etc.) properties is an active field of research in cluster science because of their possible utilization as components in nanoelectronic devices [8, 9].

In a recent paper, we have initiated a systematic study of structural and electronic properties of gold nanoclusters of intermediate size (1–1.5 nm) [10]. The lowest-energy structures of isolated Au_n (n = 38, 55, 75) clusters were determined [10] through the use of unconstrained dynamical and genetic–symbiotic (evolutive) optimization methods [11, 12]. For the three sizes investigated, which correspond to magic number clusters [13], a set of isomers nearly degenerate in energy had the lowest-energy minima of the potential energy surface (PES). Most of these cluster configurations have little or no spatial symmetry, and therefore can be classified as amorphous-like or disordered structures. Crystalline and quasicrystalline configurations were also found as local minima of the PES with similar energies to those of the disordered clusters [10].

In this paper, we report results on the structural properties as well as on the thermal stability of several isomers (ordered and disordered) of Au_{38}. A detailed theoretical study of the physical properties of this cluster is particularly interesting for several reasons. First, it is the most likely candidate for the mass spectroscopy signal with the lowest mass (8000 amu), obtained recently [3]. Clusters of this size have been structurally characterized by X-ray powder diffraction; their optical absorption spectra have been measured and show quantum size effects [3]. A cubic close-packed (fcc) structure was tentatively assigned to this cluster based on the stability advantage of the 38-atom truncated octahedral structure [3].

The main objective of this work is to obtain the distribution of lowest-energy minima that characterizes the PES of Au_{38} through dynamical and evolutive optimization methods. In addition, we study the energy ordering and structural and thermal stability properties for representative isomers (of crystalline, quasicrystalline, and disordered configurations) using semiempirical and first-principle approaches. Section 2 briefly describes the diverse

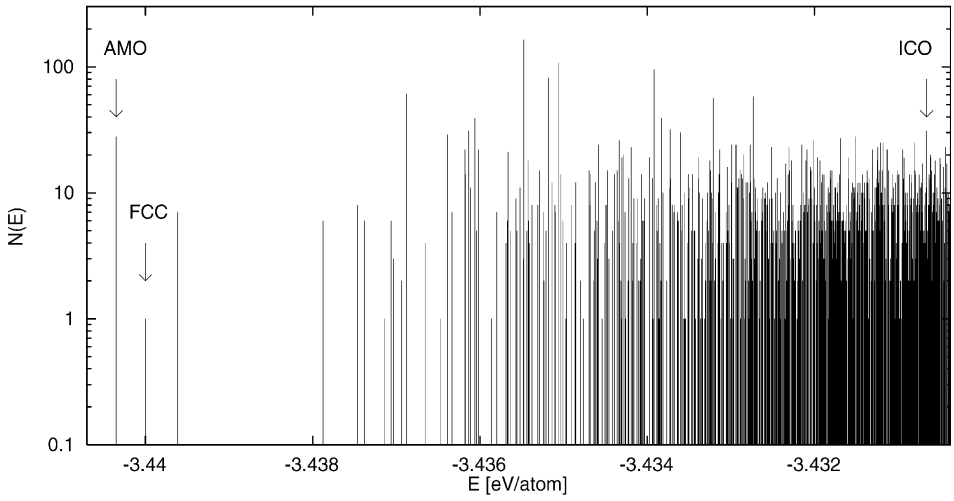

Fig. 1. Energy distribution of minima of the Au_{38} cluster. The arrows indicate the energy of the most stable amorphous, truncated octahedron and icosahedron structures.

methodologies used. The results obtained and a discussion of them are given in Sect. 3. A summary and conclusion are presented in Sect. 4.

2 Methodology

Metallic bonding in gold clusters is modeled through an n-body Gupta potential. It contains an attractive term derived from the second-moment approximation of a tight-binding model plus a repulsive pairwise Born–Mayer interaction [14]. As a function of the interatomic distances, it is written as

$$V = \frac{U_n}{2} \sum_{j=1}^{n} \left\{ A \sum_{i(\neq j)=1}^{n} \exp[-p(r_{ij}/r_{0n} - 1)] - \left(\sum_{i(\neq j)=1}^{n} \exp[-2q(r_{ij}/r_{0n} - 1)] \right)^{1/2} \right\} . \quad (1)$$

In this work, we used the values $p = 10.15$ and $q = 4.13$, which have been fitted to bulk gold [14]. The value of the parameter $A = 0.118438$ is obtained by the minimization of the cohesive energy of the fcc metal at the equilibrium value of its nearest-neighbor distance. The parameters $U_{38} = 3.63\,\text{eV}$ and $r_{038} = 2.89\,\text{Å}$ were obtained by the fitting of the cluster binding energy and average nearest-neighbor distance to first-principle results [7], using the fcc cluster structure. This potential has been used in several studies of transition- and noble-metal bulk and cluster systems. It has given an adequate representation of the n-body metallic interaction [15–17]. The similarity of this potential to other related approaches (embedded-atom method, effective medium theory, glue potential, etc.) has been widely discussed elsewhere [18].

To determine the distribution of lowest enrgy minima of the Au_{38} cluster, we used, initially, simulated annealing (SA) and simulated quenching (SQ) techniques [19]. These are global optimization methods in which no assumptions are imposed on the cluster symmetry. We carried out molecular dynamics (MD) simulations to generate the cluster trajectories. Although SA and SQ are effective global optimization methods, they are inefficient and computationally expensive, especially for large systems [10, 20]. Evolutive algorithms have been very useful in extensive searches for lowest-energy configurations of clusters with a high efficiency [11, 12, 21]. In the present study, a version of an evolutive algorithm, coupled with a conjugate gradient local optimization method [12], was implemented so that exhaustive global structure optimizations of the Au_{38} cluster using the n-body Gupta potential could be made.

Some of the lowest-energy minima (fcc, icosahedron, and amorphous isomers) found using the dynamical and evolutive optimization methods and the n-body Gupta potential were further reoptimized with a first-principle approach based on density functional theory (DFT). This provided a check on the validity of the present model potential in the calculation of cluster properties, and also allowed us to study their electronic properties [10].

We used the SIESTA program [22], which solves the standard Kohn–Sham self-consistent equations in the local density approximation (LDA). A nonlocal, norm-conserving, scalar relativistic Troullier–Martins pseudopotential [23] was used, such that 11 valence electrons per Au atom were considered. Tests of the pseudopotential, as well as the size of the basis set, were realized on Au_2 and bulk Au. An energy cutoff of the finite real-space grid [22] of 100 Ry and double-z, -s, -p, and -d orbitals were used, giving small relative errors in the dimer equilibrium distance and bulk lattice constant, as compared to their experimental values. This extended basis set and finest grid provide a higher degree of accuracy in the study of the relative stability between Au_{38} isomers.

3 Results and discussion

The distribution in energy of the most stable isomers of Au_{38} was obtained through an exhaustive global optimization using 50000 runs of a symbiotic algorithm [12, 26].

Figure 1 presents the lowest-energy region of this distribution. It shows that within an energy range of 9 meV/atom from the global minimum, approximately 550 different stable isomers were found. Most of these isomers correspond to disordered structures (including the one with the lowest energy), although the fcc truncated octahedron and the icosahedron structures were also found as local minima in this energy range. Note that for Au_{38}, we did not find a single stable ordered structure as the global minimum of the PES, well separated by an energy gap from higher-energy isomers as in other metal clusters of this or other sizes. Instead, a set of nearly degenerate isomers were found to be the most stable cluster strucutres. After a geometrical analysis and the calculation of the pair distribution function of some of these isomers, we found that most of them could be classified as amorphous-like, based on the concept introduced by Rose and Berry [24] and on the characteristic features observed in the second peak of their pair distribution functions [10, 15].

The above results were obtained from the optimization of the cluster energy by the use of a Gupta n-body potential; however, the same trends were also obtained from cluster energy minimizations by the use of other semiempirical many-body interactions like the embedded-atom and glue potentials [25]. Since these results strongly depend on the potential parameters used in the calculation [26], it was necessary to test them using a first-principle (parameter-free) method. Nevertheless, a first-principle cluster global optimization is much more expensive computationally. Our approach in this work was to make an unconstrained conjugate–gradient structural relaxation using the DFT–LDA forces. Some of the isomers with O_h and I_h symmetry and the nonsymmetric lowest-energy structure found from the classical potential were used as initial configurations. The objective was to investigate the energy ordering between crystalline (truncated octhedron), quasicrystalline (icosahedron), and the most stable disordered (amorphous-like) configurations. Although many more isomers are also local minima within the same energy range as the three considered for the first-principle calculations, some insights on the energetics between ordered and disordered structures can be obtained using these three characteristic isomers. The results obtained by DFT–LDA for the three characteristic configurations indicate that these states are degenerate within an energy of 25 meV/atom, the amorphous-like structure being the most stable. The energy ordering between the three isomers calculated using the extended basis set remains the same as that obtained previously [10], confirming the trend found through the semiempirical potential. Our results using the SIESTA program can be compared with those obtained from a scalar relativistic all-electron density functional method, reported in [7]. For example, for the fcc structure, our calculated average nearest-neighbor distance of 2.77 Å is in excellent agreement with the value of 2.78 Å obtained in [7]. Corrections to the DFT–LDA results due to the generalized gradient approximation do not change the relative binding energies of the gold isomers with respect to the LDA values [7]. In addition, structural changes after the DFT–LDA reoptimization were of the order of less than 1 % in some interatomic distances, but without changes in the average coordination number or in the average nearest-neighbor distance for the three isomers considered.

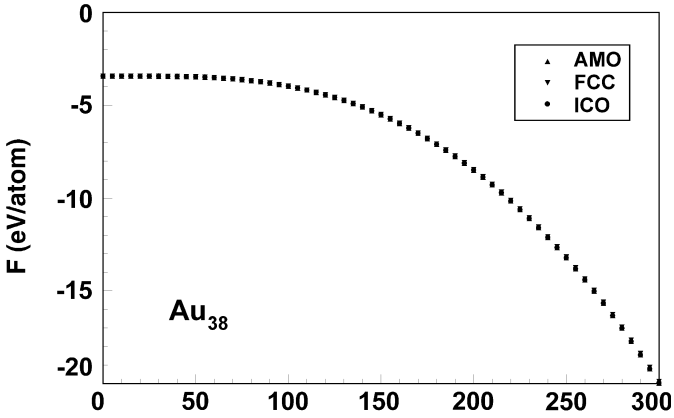

Fig. 2. Temperature dependence of the free energy per atom for the truncated octahedron (FCC), icosahedron (ICO), and amorphous (AMO) isomers of the Au_{38} cluster.

The stability of the Au_{38} isomers was studied by the use of a vibrational analysis following the calculation of their harmonic frequencies [15, 17]. A cluster configuration was considered stable if all the normal modes of all clusters in the configuration were positive. The cluster vibrational frequencies were also used to study the entropy effect, through the calculation of the cluster free energy, in the harmonic approximation [27]. Figure 2 shows the temperature dependence of the free energy per atom for the three cluster isomers. No significant differences are observed in the behavior of the free energy, and therefore none were observed in the relative thermal stability of the clusters over the temperature range studied, mainly because of the concentration of low-frequency modes in the three structures considered. The possible coexistence of different isomers at finite temperatures was studied by a constant-energy molecular dynamics simulation using the n-body Gupta potential. To detect isomerization in Au_{38}, we calculated the short-time average (over 2 vibrational periods) of the cluster kinetic energy as a function of time at several values of the cluster total energy [19].

At low total energies (or temperatures), the cluster only vibrates around its lowest-energy configuration (the amorphous-like structure). However, at intermediate total energies, coexistence between different isomers is found. At this point, where the cluster temperature is around 250 K, it has enough energy to overcome the potential barriers among different isomers and fluctuates between several structures. At higher total energies or temperatures, the cluster presents very fast changes among different configurations, corresponding to a liquid-like behavior [19].

The cluster structure factors for three different configurations are displayed in Fig. 3, together with experimental data. They were calculated using the theoretical expression for the intensity of the X-ray diffraction pattern described in [5]. These curves can be compared with the experimen-

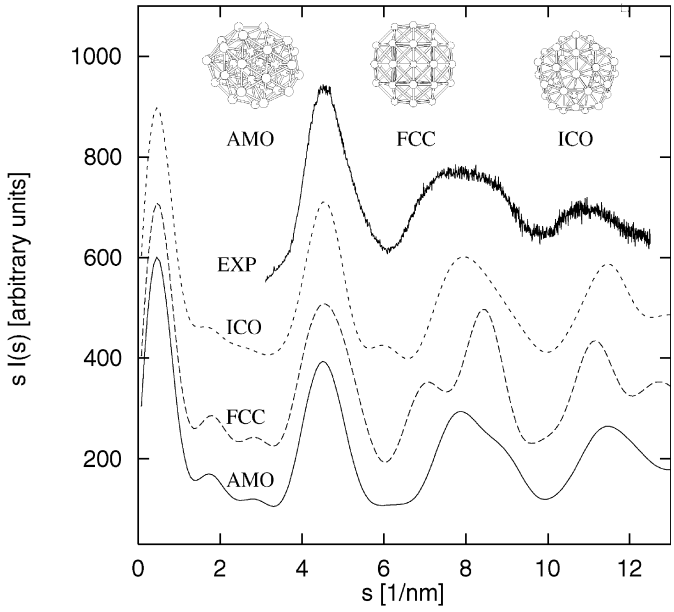

Fig. 3. Structure factors for the truncated octahedron (FCC), icosahedron (ICO), and amorphous (AMO) structures of the Au_{38} cluster. The upper curve displays the experimental data. The geometry of the three isomers is also shown.

tal X-ray diffraction pattern reported by Schaaff *et al.* [3] for the smallest gold cluster with a mass of 8000 amu. From this comparison, we conclude that the amorphous structure is in better agreement with the experimental results. The structure factors of the fcc as well as of the icosahedron configurations show additional peaks at intermediate wavelengths that are not observed in the experimental data. Nevertheless, the broad features in the experimental diffraction patterns for clusters in this size range [3] do not allow a clear discrimination of the 8000 amu structure. Future experiments with higher resolution may confirm the above predictions.

4 Summary and conclusions

A set of cluster configurations was found to have the most stable isomers (lowest-energy structures) of the Au_{38} cluster. Most of these isomers are disordered or amorphous structures, although ordered clusters (fcc and icosahedron) were also found as local minima of the PES with similar energy. These results were obtained through global optimization methods (dynamical and evolutive) using an n-body Gupta potential. The relative stability of some characteristic amorphous and ordered clusters were studied with first-principle calculations (DFT–LDA), confirming the predictions of the n-body Gupta potential.

The physical origin of this behavior can be associated with the short range of the n-body potential responsible for the metal bonding in gold clusters [10, 15, 26]. Disordered structures are possible because most of the atoms are on the cluster surface and are almost free from the constraints of bulk packing. Small changes in the positions of distant neighbors can lead to different structures. The range of the n-body interaction is related to the values of the parameters of the Gupta potential. We made similar optimizations for Ni_n and Ag_n clusters [26], which have a longer range potential. In these cases, a single ordered structure is found to be the lowest-energy configuration, with other isomers of higher energy separated by a significant gap which depends on the cluster size and potential range [26].

To confirm the predictions on the structural properties of the most stable Au_{38} isomers, it is necessary to perform X-ray powder diffraction measurements with higher resolution than is available at present. However, high-resolution transmission electron microscopy experiments have already reported images of gold and palladium nanoparticles with polycrystalline and amorphous structures in the particle size range of a few nanometers [28, 29].

Additional effort is necessary for the calculation and classification of [15] the physical properties of the large number of most stable isomers that characterize the PES of Au nanoclusters of intermediate size (1–2 nm). Work in such direction is currently in progress [25]. It is also important to note that the results presented in this work are for *isolated* Au_{38} clusters. The experimental measurements of X-ray diffraction patterns [3] were performed on passivated samples. It is still not clear what effect the passivating organic compounds have on the structure of the metallic clusters. Studies of the organometallic nanostructured materials, including those which incorporate sequences of nucleic bases to interconnect the passivated gold nanoclusters [30, 31], are being planned for the future.

This work was supported by DGSCA-UNAM Supercomputer Center, DGAPA-UNAM under Project IN101297, CONACYT, Mexico grant 25083-E, and Spain's DGES under grant PB95-0202. We thank R. Whetten for sending us the experimental data of the Au_{38} structure factor.

References

1. R.L. Whetten *et al.*: Adv. Mater. **5**, 8 (1996)
2. M.M. Alvarez *et al.*: Chem. Phys. Lett. **266**, 91 (1997)
3. T.G. Schaaff *et al.*: J. Phys. Chem. **101**, 7885 (1997)
4. W.D. Luedtke, U. Landman: J. Phys. Chem. **100**, 13 323 (1996)
5. C.L. Cleveland *et al.*: Z. Phys. D **40**, 503 (1997)
6. C.L. Cleveland *et al.*: Phys.Rev. Lett. **79**, 1873 (1997)
7. O.D. Häberlen *et al.*: J. Chem. Phys. **106**, 5189 (1997)
8. R.P. Andres *et al.*: Science **272**, 1323 (1996)
9. R.P. Andres *et al.*: Science **273**, 1690 (1996)
10. I.L. Garzón *et al.*: Phys. Rev. Lett. **81**, 1600 (1998)
11. K. Michaelian: Am. J. Phys. **66**, 231 (1998)
12. K. Michaelian: Chem. Phys. Lett. **293**, 202 (1998)
13. D.J. Wales: Science **271**, 925 (1996)
14. V. Rossato, M. Guillope, B. Legrand: Philos. Mag. A. **59**, 321 (1989)
15. I.L. Garzón, A. Posada-Amarillas: Phys. Rev. B **54**, 11 796 (1996)
16. A. Posada-Amarillas, I.L. Garzón: Phys. Rev. B **53**, 8363 (1996)

17. A. Posada-Amarillas, I.L. Garzón: Phys. Rev. B **54**, 10 362 (1996)
18. S.M. Foiles: Mater. Res. Soc. Bull. **21**, 24 (1996)
19. J. Jellinek, I.L. Garzón: Z. Phys. D **20**, 239 (1991); I.L. Garzón, J. Jellinek: Z. Phys. D **20**, 235 (1991); Z. Phys. D **26**, 316 (1993)
20. J.P.K. Doye, D.J. Wales: Phys. Rev. Lett. **80**, 1357 (1998)
21. D.M. Deaven, K.M. Ho: Phys. Rev. Lett. **75**, 288 (1995); D.M. Deaven *et al.*: Chem. Phys. Lett. **256**, 195 (1996)
22. P. Ordejón, E. Artacho, J.M. Soler: Phys. Rev. B **53**, 10 441 (1996); D. Sánchez-Portal *et al.*: Int. J. Quantum Chem. **65**, 453 (1997)
23. N. Troullier, J.L. Martins: Phys. Rev. B **43**, 1993 (1991)
24. J.P. Rose, R.S. Berry: J. Chem. Phys. **98**, 3262 (1993)
25. J.M. Soler *et al.*: to be published
26. K. Michaelian, N. Rendón, I. L Garzón: to be published
27. T.P. Martin: Phys. Rep. **95**, 167 (1983)
28. S. Tehuacanero *et al.*: Acta Metall. Mater. **40**, 1663 (1992)
29. W. Krakow, M.J. Yacamán, J.L. Aragón: Phys. Rev. B **49**, 10 591 (1994)
30. C.A. Mirkin *et al.*: Nature **382**, 607 (1996)
31. A.P. Alivisatos *et al.*: Nature **382**, 609 (1996)